# Mechanism of superconductivity in the polyhedral-network compound $Ba_8Si_{46}$

K. TANIGAKI*[1,2], T. SHIMIZU[3], K. M. ITOH[2,3], J. TERAOKA[1], Y. MORITOMO[2,4] AND S. YAMANAKA[5]

[1]Graduate School of Science, Materials Science Osaka City University, 3-3-138, Sugimoto, Sumiyoshi, Osaka 558-8585, Japan
[2]PRESTO/CREST-JST, 4-1-8 Honcho, Kawaguchi, Saitama 332-0012, Japan
[3]Department of Applied Physics and Physico-Informatics, Keio University, Yokohama 223-8522 Japan
[4]Department of Applied Physics, Nagoya University, Furo-cho, Chidane-ku, Nagoya 464-8601, Japan
[5]Department of Applied Chemistry, Hiroshima University, Higashi-Hiroshima 739-8527, Japan
*e-mail: tanigaki@sci.osaka-cu.ac.jp

Published online: 14 September 2003; doi:10.1038/nmat981

**The silicon clathrates—materials composed of metal-doped $Si_{20}$ dodecahedra—were identified as the first superconductors based on pure silicon networks[1,2]. The mechanism of superconductivity in these materials can be obtained by studying their phonon modes, as modified by isotope substitution, and specific-heat measurements. Here, we present experimental studies that provide strong evidence that superconductivity in $Ba_8Si_{46}$ is explained in the framework of phonon-mediated Bardeen–Cooper–Schriefer theory. Analyses using the McMillan approximation[3,4] of the Eliashberg equation indicate that the superconducting mechanism is in the medium coupling regime, but at the high-end limit. The large density of states at the Fermi level, which arises from hybridization of the $Si_{20}$ cluster and Ba orbitals, is responsible for the unexpectedly high superconducting temperature. The temperature evolution of the specific heat unambiguously shows that this is an s-wave symmetry superconductor.**

Syntheses with isotope elements have been key research areas for determining the mechanism of superconductivity. After what became known as the 'Woodstock time' of physics of high-superconducing-temperature ($T_c$) cuprates[5] followed by charge-transfer organic complexes[6] in the early 1980s, cluster $C_{60}$ materials have emerged as a new type of superconductor[7] with relatively high $T_c$ ranging from[8,9] 2 K to 30 K. In the mid 1990s, clathrates composed of similar pure $Si_{20}$ dodecahedra with appropriate doping were identified as the first superconductor based on pure silicon networks[1]. New-layered superconductors, HfN and $MgB_2$, have now been discovered[10,11]. Important information concerning the mechanism of superconductivity in many of these materials has been obtained by studying their phonon modes, as modified by isotope substitution, and related specific heat measurements; for cuprates[12], organic complexes[13], $C_{60}$ (refs 14–16), HfN (ref. 17), and $MgB_2$ (ref. 18). Although an unexpectedly high $T_c$ has been observed in the first pure silicon polyhedral-network $Si_{46}$ clathrates, isotope experiments have not yet been carried out.

This is because the production of sufficiently high-quality samples with accurate composition for experimental observation of the expected naive superconducting isotope shift was very difficult due to pure, stable $^{30}Si$ not being readily been available. Furthermore, it was not possible to control the stoichiometry in the $Na_2Ba_6Si_{46}$ superconductor that was first discovered[1]. Fortunately, progress in the synthesis of a new silicon-network $Ba_8Si_{46}$ superconductor under high pressure[2] has enabled precise control of the stoichiometry, and strong demand from the field of isotope engineering for semiconductors[19,20] has also spurred on efforts that have led to the successful separation of such stable Si isotopes. The combination of these developments has finally made the long-sought scientific key experiments for superconductivity using the two high-quality $Ba_8Si_{46}$ superconductors comprising of 97.97% $^{30}Si$ and 92.2% $^{28}Si$, seven years after its discovery. In this paper we report on the superconductivity isotope shift of $Ba_8Si_{46}$ together with the related

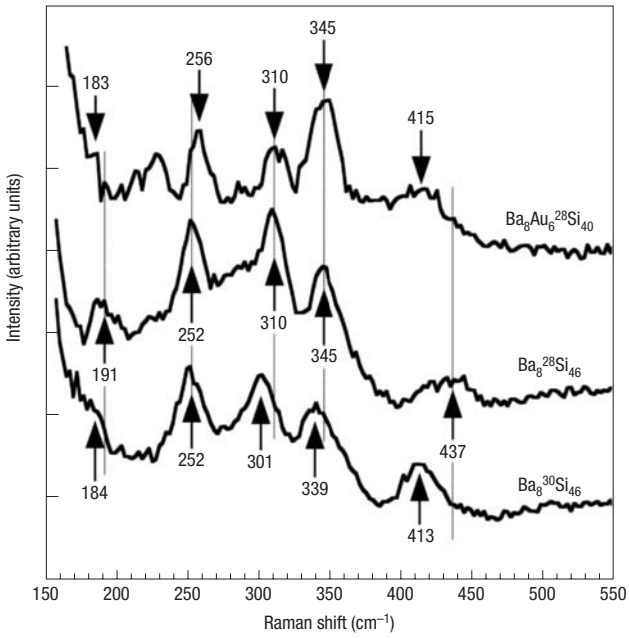


**Figure 1 Raman spectra of $Ba_8{}^{28}Si_{46}$, $Ba_8{}^{30}Si_{46}$ and $Ba_8Au_6{}^{28}Si_{40}$.** The arrows indicate the positions of vibrational peaks.

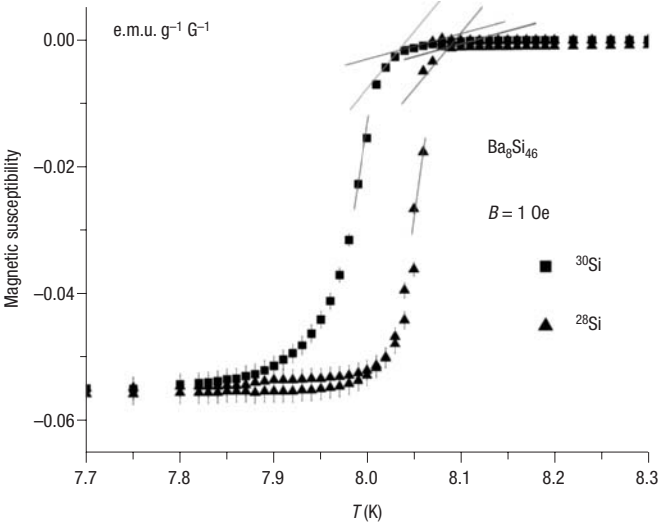


**Figure 2 Diamagnetic susceptibilities of $Ba_8{}^{30}Si_{46}$ and $Ba_8{}^{28}Si_{46}$ measured by SQUID under 1 Oe magnetic field after zero-field cooling.**

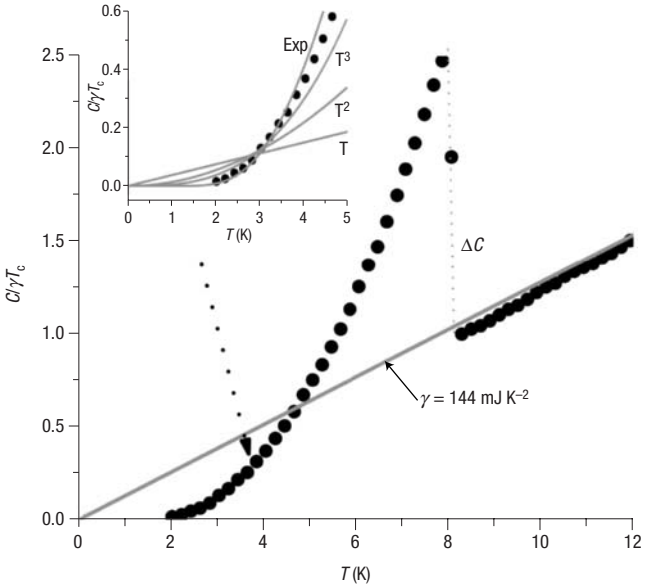


**Figure 3 The temperature evolution of the specific heat $C$ of $Ba_8Si_{46}$ scaled by $\gamma T_c$.** The inset shows the fitting curves using exponential and $T^n$ functions below the superconducting transition.

phonon modes and specific heats; all these experiments unambiguously clarify its superconductivity mechanism.

$Ba_8Si_{46}$ was synthesized from pure Ba and natural or isotopically enriched $^{30}$Si at 800 K under 3 GPa. The samples denoted as $Ba_8{}^{28}Si_{46}$ were prepared from natural-abundance Si with isotopic composition of 92.2% $^{28}$Si, 4.7% $^{29}$Si and 3.1% $^{30}$Si with an average mass 28.11, whereas the isotopic composition of $Ba_8{}^{30}Si_{46}$ is 0.82% $^{28}$Si, 1.21% $^{29}$Si and 97.97% $^{30}$Si with an average mass of 29.97. Rietveld analyses of the X-ray diffraction data measured at SPring-8 (the synchrotron source in Japan) with a Cerius2 analytical package program confirmed that both $Ba_8{}^{28}Si_{46}$ and $Ba_8{}^{30}Si_{46}$ were highly crystalline with a quality sufficient for observation of isotope effects. Structural refinement has shown $R_p$ factors and lattice constant $a_0$ values to be 4.12% and 10.328 Å for $Ba_8{}^{28}Si_{46}$, and 5.89% and 10.335 Å for $Ba_8{}^{30}Si_{46}$, in the $Pm\bar{3}n$ space group.

Room-temperature Raman spectra of $Ba_8{}^{28}Si_{46}$ and the isotopic composition $Ba_8{}^{30}Si_{46}$ are shown in Fig. 1. Five distinctive peaks at 191, 252, 310, 345 and 437 cm$^{-1}$ were observed clearly for $Ba_8{}^{28}Si_{46}$ with a Jobin Yvon T6400 spectrometer. Because these features are very similar to the previous observation[21] of the peaks at 255.9, 313.1, 345.2, 415.6, 442.1 and 453.8 cm$^{-1}$ for $Na_8{}^{28}Si_{46}$, the broad peak observed at 437 cm$^{-1}$ in the present study is considered to be deconvoluted to the three 415.6, 442.1 and 453.8 cm$^{-1}$ peaks. Among the five peaks identified for $Ba_8Si_{46}$, four at 191, 310, 345 and 437 cm$^{-1}$ show clear Si isotope shifts in the range of 0.95–0.98. These shifts are in good agreement with an estimate based on the simple harmonic approximation $(^{28}m/^{30}m)^{1/2} = 0.97$, where $^{28}m = 28.11$ and $^{30}m = 29.97$ are the average masses of Si isotope elements. In contrast, the peak at 252 cm$^{-1}$ does not show any shifts. Consequently, we can assign the four shifted peaks to the Si vibrational modes and the non-shifted peak centred at 252 cm$^{-1}$ to the Ba mode.

Considering the fact that the superconductivity is extremely depressed by a small amount of substitution of Au at the 6*c* crystal site, and only the 437 cm$^{-1}$ peak shifts by this substitution[22], it seems likely that the 437 cm$^{-1}$ phonon may play the most important role by having Cooper pairing. However, as is described later, instead of using this special phonon mode, we used the lower and the upper limits of the phonon frequencies experimentally observed ranging from 191–437 cm$^{-1}$ for analysis, to rule out the ambiguity of the associated phonon frequencies experimentally determined for discussion. The highest limit would be the 437 cm$^{-1}$ (629 K) phonon mode in the Raman data because the 521 cm$^{-1}$ of the bulk $^{28}$Si high-frequency optical phonon can be regarded as the upper bound for the $Ba_8Si_{46}$ phonons.

SQUID (semiconducting quantum interference device, Quantum Design PPMS 7) measurements with a low magnetic field of 1 Oe were used to determine $T_c$s of $Ba_8{}^{28}Si_{46}$ and $Ba_8{}^{30}Si_{46}$. As seen in Fig. 2, $T_c = 8.07$ K of $Ba_8{}^{28}Si_{46}$ decreases to $T_c = 8.02$ K for $Ba_8{}^{30}Si_{46}$ when we use the onset as the transition temperature. Taking a different criterion, such as the maximum slope or the halfway point, the shift might become slightly larger. Careful handling of the data has given a value of $\Delta T_c$ = 0.04–0.06 K. This reduction in $T_c$ value leads to the superconducting isotope coefficient of $\alpha = 0.12$–$0.23$ from the equation $\alpha = \ln(1-\Delta T_c/T_c)/\ln[M(^{28}Si_{46})/M(^{30}Si_{46})]$, where $M$ denotes the mass in the unit cell. From the fact that the value of $\alpha$ is much smaller than the expected 0.5 in Bardeen–Cooper–Schriefer (BCS) theory, we used the McMillan equation[3], one of the most useful solutions of Eliashberg's equation for interpretation:

$$T_c = [<\omega>/1.20]\exp\{-[1.04(1+\lambda)]/[\lambda-\mu^*(1+0.62\lambda)]\},$$

where the electron-boson mass-renormalization parameter $\lambda = VN_{EF}$ with the coupling constant $V$ and the density of state at the Fermi level $N_{EF}$; $\mu^*$ is the Coulomb pseudopotential. Then $\alpha$ can be extracted from $\alpha = \{\partial T_c\}/\partial \ln M\} = 0.5\{1 - [\mu^*\ln<\theta>/1.20T_c]\}^2(1 + 0.62\lambda)/(1 + \lambda\}$. Inserting the values of $T_c = 8.07$ K and $\alpha = 0.08$–$0.12$, as well as the phonon mode ranging from 191 cm$^{-1}$ (275 K) to 437 cm$^{-1}$ (629 K), experimentally estimated from our Raman analyses described earlier, into these equations, $\lambda = 0.79$–$1.2$ and $\mu^* = 0.23$–$0.31$ are obtained by these two simultaneous equations. These resulting parameters are still within the values of conventional superconductors, although the latter parameter $\mu^*$ is at the high end of the limit. It is noted that the measured isotope effect on $Si_{46}$ lattice is a partial isotope effect[4], as the Ba wavefunctions may be strongly involved in the formation of the Fermi surfaces as discussed later. Analyses including the mass of Ba modify the

estimation of $\lambda$ and $\mu^*$ to slightly smaller values within the criteria of the discussion; this factor will be interesting to study in future experiments.

To obtain more accurate information on the mechanism of superconductivity, we carried out specific-heat measurements from room temperature to 2 K on $Ba_8Si_{46}$ having a natural abundance of $^{28}Si$. The experimental data were analysed using both the Debye and Einstein terms. In particular, the important Sommerfeld parameter $\gamma$ and the low-temperature phonon coefficient $A$ were obtained by handling the data in a standard method using $C/T = \gamma + AT^2$, where $C$ is the specific heat capacity, at low temperatures. The Debye temperature of $\theta_D = 370$ K was extracted from $A = 2.04$ mJ mol$^{-1}$ K$^{-4}$. From the observed $\gamma$ value of 144 mJ mol$^{-1}$ K$^{-2}$, the density of states at the Fermi level $N_{EF}$ can be estimated to be 31 states per eV per $Si_{46}$-unit from the relationship of $N_{EF} = 3\gamma/2\pi^2 k_B^2$, where $k_B$ is Boltzmann's constant, which is higher than those of $A_3C_{60}$ van der Waals-type cluster superconductors ranging generally from 10–20 states per eV per $C_{60}$-unit.

The density of states, $N_{EF}$, at the Fermi level of $Ba_8Si_{46}$ has also been estimated from the magnetic susceptibility measurements using SQUID. Assuming that the orbital diamagnetic susceptibility (Landau part) is quenched, subtraction of the core-level diamagnetic part $\chi_{dia} = -3.2 \times 10^{-7}$ e.m.u. g$^{-1}$ (estimated from the experimental value of the diamagnetic $Ba_8Cu_4Si_{42}$) from the total magnetic susceptibility $\chi_{total}$ leads to the Pauli paramagnetic susceptibility $\chi_{Pauli} = 8.0 \times 10^{-7}$ e.m.u. g$^{-1}$. From this estimate, $N_{EF}$ is determined to be 28 states per eV per $Si_{46}$-unit, being in good agreement with the result of specific-heat measurements. Actually, the Wilson factor $R = [\pi^2 k_B^2/(3\mu_B^2)][\chi_{Pauli}/\gamma]$ is 0.9, and this suggests that electron–electron correlations are not very strong in this material.

The jump at the superconducting transition temperature shows an apparent energy gap under the superconducting state, and the change in the scaled value of $\Delta C/(\gamma T_c)$ at the transition temperature, as well as the evolution of heat capacity as a function of temperature after the superconducting transition, supplies important information about the nature of the superconducting mechanism. As shown in Fig. 3, the scaled specific heat capacity jump is 1.52 and this is slightly larger than the expected value of 1.43 from the weak coupling BCS theory, but not far from those of other conventional superconductors such as Hg, Pb and $Nb_3Sn$. The temperature evolution of the specific heat after the superconducting transition follows the exponential decay as seen in the inset of Fig. 3, and this shows that $Ba_8Si_{46}$ is categorized as an s-wave superconductor. The $2\Delta$ energy gap can also be estimated to be 5 meV and its scaled value of $2\Delta/(k_B T_c)$ is 3.60, being very close to the upper limit of 3.52 from the conventional BCS theory.

So far, two types of polyhedra-network systems have been reported for superconductors; one is the covalent-network $Si_{46}$ and the other the van der Waals-network $C_{60}$ polyhedra. Therefore, it is worthwhile to compare the features between these two superconductors. As was described, the situation observed in this covalent-network material is different from the one encountered for the van der Waals-network type $C_{60}$ superconductors. The striking contrast is the configuration of the wave functions constructing the Fermi surface. As was suggested by X-ray absorption and emission experiments[23] and band caluculations[24], the high $N_{EF}$ value in $Ba_8Si_{46}$ is ascribed to the band modification through hybridization of Ba $5p/5d$ orbitals with dodecahedra $Si_{20}$ cluster orbitals. Only alkali metal (A)-doping does not lead $A_8Si_{46}$ to a superconducting state. On the other hand, the scenario of the $C_{60}$ superconductivity is based on the role of the triply degenerate pure $t_{1u}$-derived $C_{60}$ band, which can change a Mott insulating state with relatively large on-site Coulomb repulsion energy to a metallic state with high $N_{EF}$. As a result, the hybridization with Ba orbitals loses this intrinsic characteristic by broadening the band width, in turn reducing $T_c$ values.

Received 3 June 2003; accepted 15 August 2003; published 14 September 2003.

## References


1. Kawaji, A. Horie, H., Yamanaka, S. & Ishikawa, M. Superconductivity in the silicon clathrate compound (Na,Ba)$_x$Si$_{46}$. *Phys. Rev. Lett.* **47,** 1427–1429 (1995).
2. Yamanaka, S., Enishi E., Fukuoka, H. & Yasukawa, M. High-pressure synthesis of a new silicon clathrate superconductor $Ba_8Si_{46}$. *Inorg. Chem.* **39,** 56–58 (2000).
3. McMillan, W. L. Transition temperature of strong-coupled superconductors. *Phys. Rev.* **167,** 331–344 (1968).
4. Carbotte, J. P. Properties of boson-exchange superconductors. *Rev. Mod. Phys.* **62,** 1027–1157 (1990).
5. Bednorz, J. G. & Müller, K. A. Possible high T$_c$ superconductivity in the Ba-La-Cu-O system. *Z. Phys. B Condens. Matter* **64,** 189–193 (1986).
6. Jèrome, D., Mazaud, A., Ribauld, M. & Bechgaad, K. Superconductivity in a synthetic organic conductor $(TMTSF)_2PF_6$. *J. Physique Lett.* **41,** L95–L98, (1980).
7. Hebard, A. F. *et al.* Superconductivity at 18 K in potassium-doped $C_{60}$. *Nature* **350,** 600–601 (1991).
8. Tanigaki, K. *et al.* Superconductivity at 33 K in $Cs_xRb_yC_{60}$. *Nature* **352,** 222–223 (1991).
9. Tanigaki, K. *et al.* Superconductivity in sodium- and lithium-containing alkali-metal fullerides, *Nature* **356,** 419–421 (1992).
10. Yamanaka, S., Hotehama, K. & Kawaji, H. Superconductivity at 25.5 K in electron-doped layered hafnium nitride. *Nature* **392,** 580–582 (1998).
11. Nagamatsu, J., Nakagawa, N., Muranaka, T., Zenitani, Y. & Akimitsu, J. Superconductivity at 39 K in magnesium diboride. *Nature* **410,** 63–64 (2001).
12. Bourne, L. C., Zettle, A., Barbee, T. W. III & Cohen. M. L. Complete absence of isotope effect in $YBa_2Cu_3O_7$. *Phys. Rev. B.* **36,** 3990–3993 (1987).
13. Williams, J. M. *et al.* Organic superconductors new benchmarks. *Science* **252,** 1501–1503 (1991).
14. Ebbesen, T. W. *et al.* Isotope effect on superconductivity in $Rb_3C_{60}$. *Nature* **335,** 620–622 (1992).
15. Ramirez, A. P. *et al.* Isotope effect in superconducting $Rb_3C_{60}$. *Phys. Rev. Lett.* **68,** 1058–1061 (1992).
16. Fuhrer, M. S., Cherrey, K., Zettle, A., Cohen, M. L. &. Crespi, V. H. Carbon isotope effect in single-crystal $Rb_3C_{60}$. *Phys. Rev. Lett.* **83,** 404–407 (1999).
17. Tou, H., Maniwa, T. & Yamanaka, S. Superconducting characteristics in electron-doped layered hafnium nitride: $^{15}N$ isotope effect studies. *Phys. Rev. B* **67,** 100509 (2003).
18. Petrovic, C. *et al.* Boron isotope effect in superconducting $MgB_2$. *Phys. Rev. Lett.* **86,** 1877–1899 (2001).
19. Haller, E. E. Isotopically engineered semiconductors. *J. Appl. Phys.* **77,** 2857–2878 (1995).
20. Takyu, K., Itoh, K. M., Oka, K., Saito, N. & Ozhogin, V. I. Growth and characterization of the isotopically enriched $^{28}Si$ bulk single crystal. *Jpn J. Appl. Phys.* **38,** L1493–L1495, (1999).
21. Fang, S. L. *et al.* Raman scattering from vibrational modes in $Si_{46}$ clathrates. *Phys. Rev. B* **57,** 7686–7693 (1998).
22. Herrmann, R., Tanigaki, K., Kawaguchi, T., Kuroshima, S. & Zhou, O. Electronic structure of Si and Ge gold-doped clathrates. *Phys. Rev. B* **60,** 13245–13248 (1999).
23. Yokoya, T. *et al.* Electronic structure and superconducting gap of silicon clathrate $Ba_8Si_{46}$ studied with ultrahigh-resolution photoemission spectroscopy. *Phys. Rev. B* **64,** 172504 (2001).
24. Saito, S. & Oshiyama, A. Electronic Structure if $Si_{46}$ and $Na_2Ba_6Si_{46}$. *Phys. Rev. B* **51,** 2628–2631 (1995).


## Acknowledgements

The authors thank V. I. Ozhogin for supplying $^{30}Si$ and T. Atake for discussion of specific heat. We also wish to thank the staff members at SPring-8, Japan (beamline BL02B2 and BL25SU) for their support and to express our appreciation for the use of the facility of high-energy beam. Institute of Material Research No129-2003 is also acknowledged for support of its facility usage. Financial support from the nanotechnology proposals of the both beam lines from SPring-8 is also greatly appreciated. The project was supported by a Grant-in-Aid from the Ministry of Education, Sport, Science and Culture of Japan, No. 13304031 and 14076215. This work has been supported by PRESTO and CREST of JST (Japan Science and Technology Corporation).
Correspondence and requests for materials should be addressed to K.T.

## Competing financial interests

The authors declare that they have no competing financial interests.